



Characterization of reactive nitrogen in the global upper troposphere using recent and historic commercial and research aircraft campaigns and GEOS-Chem

5 Nana Wei¹, Eloise A. Marais¹, Gongda Lu^{1*}, Robert G. Ryan^{1**}, Bastien Sauvage²

¹Department of Geography, University College London, London, UK.

²Laboratoire d'Aérodynamique, Université de Toulouse, CNRS, Université Toulouse III Paul Sabatier, France.

* Now at: the Satellite Application Centre for Ecology and Environment (SACEE), Beijing, China.

10 ** Now at: School of Geography, Earth and Atmospheric Science, University of Melbourne, Melbourne, Australia.

Correspondence to: Nana Wei (nana.wei.21@ucl.ac.uk); Eloise A. Marais (e.marais@ucl.ac.uk)

Abstract. Reactive nitrogen (NO_y) in the upper troposphere (UT; ~8-12km) influences global climate, air quality, and tropospheric oxidants, but this is informed by limited knowledge of the relative contribution of individual NO_y components in this undersampled layer. Here we use sporadic NASA DC-8 aircraft campaign observations, after screening for plumes and stratospheric influence, to characterise UT NO_y composition and evaluate current knowledge of UT NO_y as simulated with the GEOS-Chem model. Use of DC-8 data follows confirmation that these sporadic data reproduce NO_y seasonality from routine commercial aircraft observations (2003-2019), supporting use of DC-8 data to characterize UT NO_y. We find that peroxyacetyl nitrate (PAN) dominates UT NO_y (30-64% of NO_y), followed by nitrogen oxides (NO_x ≡ NO + NO₂) (6-18%), peroxyacetic acid (HNO₄) (6-13%), and nitric acid (HNO₃) (7-11%). Methyl peroxy nitrate (MPN) makes an outsized contribution to NO_y (24%) over the Southeast US relative to the other regions sampled (2-7%). GEOS-Chem, sampled along DC-8 flights, exhibits much weaker seasonality than DC-8, underestimating summer and spring NO_y and overestimating winter and autumn NO_y. The model consistently overestimates peroxypropionyl nitrate (PPN) by up to 16 pptv and underestimates NO₂ by 6-36 pptv, as the model is missing PPN photolysis. An ~80 pptv (20-fold) underestimate in modelled MPN over the Southeast US results from uncertainties in processes that sustain MPN production as air ages. Our findings highlight that greater understanding of UT NO_y is critically needed to determine its role in the nitrogen cycle, air pollution, climate, and abundance of oxidants.

1 Introduction

Reactive nitrogen (NO_y) in the upper troposphere (~8-12 km) impacts global climate, surface air quality and the oxidizing capacity of the whole troposphere (Bradshaw et al., 2000; Dahlmann et al., 2011; Mickley et al., 1999; Worden et al., 2011). NO_y is an important climate driver because tropospheric ozone (O₃) production is limited by the availability of NO_y, particularly in the upper troposphere where the radiative forcing efficiency of O₃ peaks (Dahlmann et al., 2011; Rap et al., 2015; Worden et al., 2011). Influence on tropospheric O₃ production also affects abundance of the main atmospheric oxidant, the hydroxyl radical (OH), thus altering the lifetimes of the longer-lived greenhouse gas methane and the air pollutants carbon monoxide (CO) and volatile organic compounds (VOCs) (Murray et al., 2013; Seltzer et al., 2015).



Knowledge of dominant daytime NO_y compounds, sources, chemistry, fate, and persistence in the upper troposphere has been largely informed by observations and models used as part of research and commercial aircraft campaigns (Boersma et al., 2011; Marais et al., 2018; Silvern et al., 2018; Travis et al., 2020; Travis et al., 40 2016). Instruments onboard research aircraft that sample the upper troposphere, in particular the recently retired NASA DC-8 platform, have undergone substantial development to directly measure and derive estimates of a large suite of upper tropospheric NO_y compounds. These include nitrogen oxides ($\text{NO}_x \equiv \text{NO} + \text{NO}_2$), peroxyacetyl nitrate (PAN) and other prominent PAN-type compounds, nitric acid (HNO_3), peroxyxynitric acid (HNO_4), alkylnitrates (ALKNs) and, more recently, methyl peroxy nitrate (MPN).

45 These aircraft campaigns have confirmed that sources of NO_y to the upper troposphere are dominated by lightning NO_x emissions (Marais et al., 2018; Levy Ii et al., 1999; Gressent et al., 2016; Gressent et al., 2014), causing a seasonal maximum in NO_y in summer months and a minimum in winter in parts of the world such as the northern midlatitudes where there is large seasonal variability in lightning activity (Stratmann et al., 2016; Blakeslee et al., 2014). Other NO_y source contributors include NO_x emissions from cruising altitude aircraft (Brasseur et al., 1996), 50 stratospheric downwelling of air masses laden with HNO_3 and NO_2 that also promote prompt formation of PANs on mixing with cold upper tropospheric air (Liang et al., 2011; Jacob et al., 2010; Levy Ii et al., 1980), deep convective uplift of surface pollution (Ehhalt et al., 1992; Jaeglé et al., 1998; Bertram et al., 2007), and aged air masses initially very photochemically active that accumulate MPN (Nault et al., 2015).

Chemical cycling of dominant daytime NO_y components in the upper troposphere is illustrated in Figure 1. During 55 the day, NO and NO_2 are in photostationary steady state, as NO oxidation, mostly by O_3 , is balanced by NO_2 photolysis. NO_x also reacts to form reservoir compounds. For NO_2 , these include HNO_3 from reaction with OH , PANs from reaction with peroxy acyl radicals ($\text{RC}(\text{O})\text{OO}$), HNO_4 from reaction with the hydroperoxyl radical (HO_2), and MPN from reaction with the methyl peroxy radical (CH_3O_2). PANs in the upper troposphere are typically dominated by PAN followed by peroxypropionyl nitrate (PPN) (Roberts, 1990; Roberts et al., 1998; 60 Roberts et al., 2002; Singh, 1987). For NO , reservoir compounds include ALKNs from reaction with non-acyl peroxy radicals (RO_2). Recycling of reservoir compounds back to NO_x is dominated by photolysis, as thermally labile peroxy nitrates (PNs) including PANs, HNO_4 and MPN are stable against decomposition in the cold upper troposphere. This recycling along with NO_y sources to the upper troposphere sustains upper tropospheric NO_x concentrations at ~ 30 pptv over the remote ocean and ~ 100 pptv over polluted landmasses (Shah et al., 2023; 65 Marais et al., 2018; Marais et al., 2021). Stable NO_x reservoir compounds are transported long distances before subsiding and decomposing on warming, thus supplying other parts of the world with oxidants (HO_x) and O_3 precursors (NO_x and peroxy radicals). Loss processes in the dry upper troposphere are slow and dominated by subsidence. In the upper troposphere, NO_y has a lifetime of 10-20 days (Logan, 1983; Prather and Jacob, 1997) and NO_x has a lifetime of about a week compared to less than a day in the boundary layer (< 2 km) (Jaeglé et al., 70 1998).

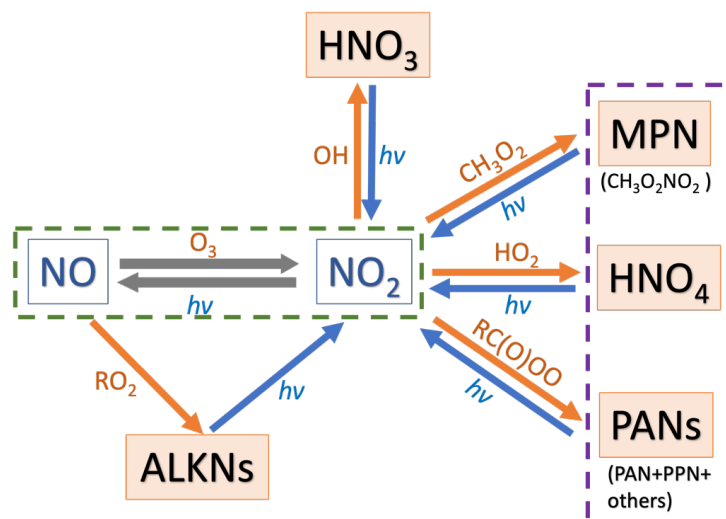


Figure 1: Dominant daytime reactive nitrogen components and reaction pathways in the upper troposphere. Arrow colours distinguish formation (orange) and photolytic ($h\nu$) decomposition (blue) of reservoir compounds. Dashed boxes indicate compounds of the NO_x family (green) and classed as peroxy nitrates (purple). "R" in RC(O)OO and RO_2 represents an alkyl group.

75 Modelling studies evaluating best understanding of NO_y in the upper troposphere routinely identify stark discrepancies between observed and modelled total NO_y , NO_x , and the ratio of NO -to- NO_2 in the upper layers of the troposphere. These studies have either focused on a few NO_y components, or a single aircraft campaign (Talbot et al., 1999; Lee et al., 2022; Bertram et al., 2007; Huntrieser et al., 2016; Liang et al., 2011; Nault et al., 2015; Fisher et al., 2018; Cohen et al., 2023). A more holistic investigation of all NO_y components is needed, as is advocated by Murray et al. (2021), to reduce uncertainties in knowledge of the current, past, and potential future abundances of tropospheric oxidants. Past studies have also documented the challenges examining measurements made in the upper troposphere. These include screening for stratospheric influence, determining the height of the chemical tropopause, and selecting observations and campaigns that are climatologically representative of a standard atmosphere (Barth et al., 2015; Fuelberg et al., 2000; Bertram et al., 2007; Huntrieser et al., 2016; Weinheimer et al., 1994). Instruments measuring NO_2 are also susceptible to interference from decomposition of the least thermally stable NO_x reservoir compounds, HNO_4 and MPN, that are abundant in the cold upper troposphere (Shah et al., 2023; Ryerson et al., 2000). NO_y from these same instruments can also be biased by decomposition of non- NO_y fixed nitrogen compounds prevalent in the upper troposphere, such as hydrogen cyanide (HCN) (Bradshaw et al., 1998).

85 Here we use NASA DC-8 research and IAGOS commercial aircraft campaign measurements, each spanning more than a decade, to characterize global NO_y seasonality and composition in the upper troposphere. This follows careful campaign and data selection to isolate observations sampling the upper troposphere under standard conditions and broad assessment of consistent NO_y seasonality between DC-8 and routine commercial aircraft campaign observations. We go on to use the DC-8 data to critique contemporary understanding of upper tropospheric NO_y as simulated by the GEOS-Chem model.



2 Materials and methods

2.1 Research aircraft observations of total and components of NO_y

100 The DC-8 research aircraft has sampled ambient air covering the full extent of the troposphere since its maiden
campaign in 1985 (Culter, 2009). Many of the initial campaigns included instruments that measured a subset of
the NO_y components shown in Figure 1, typically continuous measurements of total NO_y, NO, HNO₃, PAN and
PPN, and whole air sampler (WAS) collection and laboratory detection of C1-C5 ALKNs (Singh et al., 1999).
105 Since 2004, DC-8 campaigns have included continuous measurements of HNO₄, other PAN-type species and total
PNs. Given this, we only consider DC-8 campaigns with a relatively consistent suite of instruments that mostly
sampled well-mixed air representative of a climatologically standard atmosphere and that have limited influence
from stratospheric air. These criteria eliminate the summer 2004 Intercontinental Chemical Transport Experiment-
North America (INTEX-NA) campaign (Singh et al., 2006; Singh et al., 2009) that is the only DC-8 campaign
since 2004 to not include a NO_x and NO_y chemiluminescence analyzer, and the summer 2012 Deep Convective
110 Clouds and Chemistry (DC3) campaign that targeted convective thunderstorms influenced by fresh surface
pollution and lightning NO_x emissions (Barth et al., 2015).

The DC-8 campaigns we use are the Arctic Research of the Composition of the Troposphere from Aircraft and
Satellites (ARCTAS) over the Arctic and sub-Arctic in spring and summer 2008 (Jacob et al., 2010), the Studies
of Emissions and Atmospheric Composition, Clouds and Climate Coupling by Regional Surveys (SEAC⁴RS) over
115 the Southeast US in late summer and early autumn 2013 (Toon et al., 2016), the Korea-United States Air Quality
(KORUS-AQ) over South Korea in late spring and early summer 2016 (Crawford et al., 2021), and the
Atmospheric Tomography Mission (ATom) that included 4 sub-campaigns along the same flight path from pole
to pole over the Atlantic and Pacific Oceans in all 4 seasons from 2016 to 2018 (Thompson et al., 2021). ATom
sub-campaigns are ATom-1 in July-August, ATom-2 in January-February, ATom-3 in September-October and
120 ATom-4 in April-May. The data for these campaigns are from NASA data portals for each campaign downloaded
as merged 1-minute files for ARCTAS (NASA, 2009), SEAC⁴RS (NASA, 2015) and KORUS-AQ (NASA, 2017)
and as two separate merged files for ATom with the WAS C1-C5 ALKNs data at variable time intervals of 40 s,
1 min and 2 min and without the WAS C1-C5 ALKNs data at 1-minute resolution (NASA, 2021).

Figure 2 shows the global sampling extent of the upper troposphere by NASA DC-8 after applying filtering criteria
125 to the data to isolate observations representative of photochemical steady-state conditions. For this, we select
daytime (08h30-15h30 local solar time or LST) observations within a wide pressure range of 180 to 450 hPa (~8-
12 km) to cover the full vertical extent of the upper troposphere that varies with season and latitude. We separate
the stratosphere from the troposphere with a tropopause definition that can be applied to all datasets. We remove
data with observed O₃ concentrations above thresholds that represent the location of the chemical tropopause
130 (Zahn et al., 2002). The thresholds we use are a single year-round value for the tropics (20°N to 20°S) of 100 ppbv
(Dameris, 2015) and seasonally varying values everywhere else calculated using the day-of-year dependent O₃
tropopause equation derived by Zahn et al. (2002) from the inverse relationship between O₃ and CO observations
from commercial aircraft campaigns. These are 120 ppbv in spring, 103 ppbv in summer, 74 ppbv in autumn, and
91 ppbv in winter. We also screen for stratospheric intrusions (identified as observations with O₃/CO > 1.25 mol



135 mol⁻¹) (Hudman et al., 2007), fresh NO_x emissions (NO_y/NO < 3 mol mol⁻¹), fresh convection (large (> 10 nm
diameter) condensation nuclei > 10⁴ cm⁻³), biomass burning plumes (CO > 200 ppbv and acetonitrile > 200 pptv)
(Shah et al., 2023), as well as instances where NO₂ photolysis frequencies are approximately zero. The latter
removes high latitude ATom measurements obtained at 08h30-15h30 LST under dark conditions during polar
twilight or polar night. The data that are retained correspond to solar zenith angles ≤ 80° in polar regions, and ≤
140 60° at other latitudes.

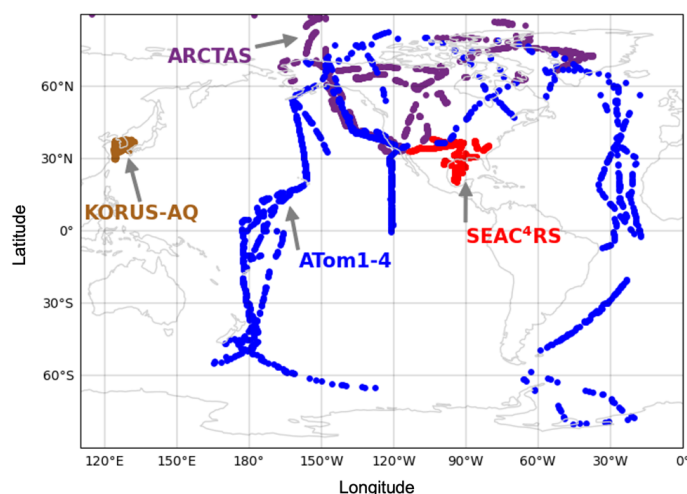


Figure 2: Extent of NASA DC-8 sampling of the upper troposphere under standard, steady-state conditions. Colours distinguish ARCTAS (plum), SEAC⁴RS (red), KORUS-AQ (brown), and ATom (blue). ATom points are the 1-minute resolution data.
145

The DC-8 instruments measuring NO_y components (Figure 1) that are common to all campaigns include a chemiluminescence instrument measuring NO, NO₂, and total NO_y (Ryerson et al., 2000; Pollack et al., 2010; Bourgeois et al., 2022), a chemical ionization mass spectrometer (CIMS) measuring HNO₃ (Crouse et al., 2006), a CIMS measuring HNO₄, PAN, PPN, and other PANs (Slusher et al., 2004), and a Whole Air Sampler (WAS)
150 collecting samples analysed in the laboratory using gas chromatography with flame ionization and atomic emission to detect C1-C5 ALKNs (Blake et al., 2003). The other PANs measured with the CIMS include peroxyacryloyl nitrate (APAN), peroxyisobutryl nitrate (PiBN), peroxybutyryl nitrate (PBN), and peroxybenzoyl nitrate (PBZN). Other instruments deployed for select campaigns are Thermal-Dissociation Laser Induced Fluorescence (TD-LIF) measuring NO₂, total PNs and total ALKNs (ARCTAS, KORUS-AQ, SEAC⁴RS) and the
155 PAN and Trace Hydrohalocarbon ExpeRiment (PANTHER) instrument measuring PAN (ATom). There are also TD-LIF methyl peroxy nitrate (MPN) measurements reported in the SEAC⁴RS dataset and derived for ARCTAS by Browne et al. (2011).

Concentrations of NO₂ in the upper troposphere are close to chemiluminescence instrument uncertainty (Pollack et al., 2010; Bourgeois et al., 2022) and the measurements include interference from decomposition of NO_x
160



reservoir compounds in the instrument inlet. The Reed et al. (2016) temperature-dependent inlet temperature decomposition profiles of individual NO_x reservoir compounds for an instrument similar to that operated on the DC-8 suggests interference of 80-100% MPN and 15-45% HNO₄ for the typical inlet temperature range of the DC-8 chemiluminescence instrument of 20-30°C (Bourgeois et al., 2022). For the campaigns that measured HNO₄ and derived or measured MPN, this amounts to 13-27 pptv for ARCTAS and 71-92 pptv for SEAC⁴RS. Given this, we instead calculate NO₂ using the NO-NO₂ photochemical steady state (PSS) approximation, as is now standard (Horner et al., 2024; Shah et al., 2023; Travis et al., 2016). Conversion of NO to NO₂, mostly (75%) due to oxidation by O₃ in the upper troposphere (Silvern et al., 2018), is balanced by NO₂ photolysis back to NO:



As NO_x is in steady state for the daylight observations we isolate, NO₂ can be calculated as follows:

$$175 \quad \text{NO}_2 = \text{NO} \times \left(\frac{k_1[\text{O}_3] + k_2[\text{HO}_2] + k_3[\text{BrO}]}{j_{\text{NO}_2}} \right) \quad (1).$$

Compounds in square brackets are in molecules cm⁻³. NO and NO₂ are in pptv. Terms not introduced yet include the NO₂ photolysis frequency, j_{NO_2} , in s⁻¹ and bromine monoxide (BrO), and rate constants of NO oxidation (R1) (k_{1-3}), are in cm³ molecule⁻¹ s⁻¹. Temperature-dependent values of k_{1-3} are those recommended by the Jet Propulsion Laboratory (JPL) (Burkholder, 2020), calculated using DC-8 ambient temperature measurements. NO, [O₃], and j_{NO_2} are from the DC-8 measurements and [HO₂] is from the DC-8 measurements for all campaigns, except SEAC⁴RS when it was not measured. We use GEOS-Chem (detailed in Sect. 2.3) simulated [HO₂] to estimate SEAC⁴RS PSS NO₂. [BrO] is from GEOS-Chem for all campaigns. NO is also converted to NO₂ by organic peroxy radicals (RO₂), but we ignore this reaction as it is relatively insignificant in the upper troposphere (Shah et al., 2023).

2.2 Commercial aircraft observations of total NO_y

We use routine observations of upper tropospheric total NO_y from instruments on commercial long-haul passenger aircraft to determine if the intermittency and brevity of DC-8 campaign observations are representative of climatological conditions. The In-service Aircraft for a Global Observing System (IAGOS) European research infrastructure (<https://www.iagos.org>, last accessed May 2024) provides routine in situ measurements of NO_y (Petzold et al., 2015). These are available from two IAGOS programmes: the Measurement of Ozone and Water Vapor by Airbus In-Service Aircraft (MOZAIC) (Marenco et al., 1998) from 2001 to 2005 (Volz-Thomas et al., 2005) and the Civil Aircraft for the Regular Investigation of the Atmosphere Based on an Instrument Container (CARIBIC) since December 2004 (Stratmann et al., 2016; Brenninkmeijer et al., 2007).

We consider the MOZAIC and CARIBIC observations together (collectively named IAGOS), as both programmes employed a chemiluminescence instrument with the same NO_y detection technique (Brenninkmeijer et al., 2007;



200 Volz-Thomas et al., 2005). Direct intercomparison of NO_y is not possible, as there is no overlap in MOZAIC and
CARIBIC NO_y . Data from 2003 to 2019 are used; 2003-2005 for MOZAIC and 2005-2019 for CARIBIC. We
isolate upper tropospheric observations by applying the same O_3 tropopause, stratospheric O_3 intrusion, and
daytime filtering as is applied to DC-8 data (Sect. 2.1). We do not screen for observations impacted by fresh
emissions, vertical convection or biomass burning plumes, due to unavailability of concurrent measurements of
205 suitable chemical tracers in the IAGOS data. As we consider 17 years of IAGOS data, we assume that the influence
of these is dampened in the long-term median of NO_y . Both the IAGOS and DC-8 data are gridded to the same 2°
latitude \times 2.5° longitude grid.

2.3 The GEOS-Chem Model

210 We use the GEOS-Chem global 3D chemical transport model version 13.0.2
(<https://doi.org/10.5281/zenodo.4681204>; last accessed May 2021) to represent contemporary understanding of
upper tropospheric NO_y for comparison to DC-8. The model is driven with consistent NASA Modern-Era
Retrospective analysis for Research and Applications version 2 (MERRA-2) assimilated meteorology at $2^\circ \times 2.5^\circ$
(latitude \times longitude) over 47 vertical layers from the surface of the Earth to 0.01 hPa. The model emissions local
215 to the upper troposphere include cruising altitude aircraft from the Aviation Emissions Inventory Code (AEIC)
(Stettler et al., 2011) and lightning emissions as described in Murray et al. (2012). Surface emissions of NO_x and
VOCs precursors of ALKNs and PNs are from the anthropogenic Community Emissions Data System (CEDS)
inventory of Hoesly et al. (2018), the Model of Emissions of Gases and Aerosols from Nature (MEGAN) biogenic
VOCs inventory version 2.1 (Guenther et al., 2012), the soil NO_x emission inventory of Hudman et al. (2012),
220 and the Global Fire Emissions Database version 4 with small fires (GFED4s) for open burning of biomass (Giglio
et al., 2013). Wet deposition of gas-phase HNO_3 , the terminal sink for NO_y subsiding from the upper troposphere,
includes in-cloud (rainout) and above-cloud (washout) scavenging as detailed in Amos et al. (2012) and enhanced
scavenging as described by Luo et al. (2020).

We sample the model at the same time and location as the DC-8 observations using the ObsPack diagnostic
225 (<https://www.esrl.noaa.gov/gmd/ccgg/obspace/>; last accessed 23 October 2024) following a minimum 10-month
spin-up preceding each campaign to initialize chemistry and large-scale circulation throughout the troposphere.
Modelled components of NO_y include NO, NO_2 , HNO_3 , HNO_4 , PAN, PPN, peroxyacetyl nitrate (MPAN),
MPN, and ALKNs.

3 Results and Discussion

230 3.1 DC-8 campaign NO_y seasonality and budget closure

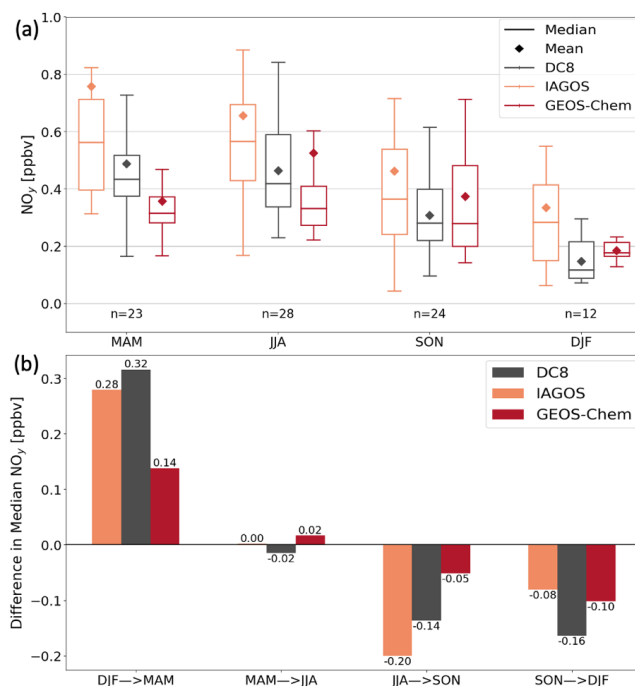
Figure 3 compares seasonality in UT NO_y from IAGOS and DC-8. Most of the overlap is with ATom along the
North Atlantic flight corridor in all seasons, ARCTAS over the Canadian Arctic and Greenland in March-May
(MAM) and June-August (JJA), and SEAC⁴RS over the Southeast US in September-November (SON). IAGOS
 NO_y exhibits similar peaks in spring (563 pptv) and summer (565 pptv), due to intensive seasonal lightning in the



235 northern hemisphere (Stratmann et al., 2016). Decline in this source decreases NO_y in autumn to 365 pptv and
 240 NO_y further decreases in winter to an annual minimum of 284 pptv.

DC-8 NO_y seasonality is similar to that of IAGOS, though the magnitude of DC-8 NO_y is consistently on average
 ~130 pptv (range of 80 pptv in SON to 170 pptv in DJF) less than IAGOS NO_y in all seasons. The ~130 pptv
 240 greater IAGOS NO_y likely results mostly from differences in sampling altitudes. The mean sampling altitude of
 IAGOS for all coincident $2^\circ \times 2.5^\circ$ grid cells is ~240 hPa (~10 km), whereas the sampling altitude for DC-8 is on
 average ~1.5 km below that of IAGOS at ~360 hPa. According to the DC-8 measurements, NO_y is ~100 pptv
 245 more at 240 hPa (IAGOS) than at 360 hPa (DC-8 mean altitude). Another minor factor may be IAGOS NO_y
 instrument interference from HCN. The IAGOS chemiluminescence instruments use a hydrogen (H_2) reagent to
 convert oxygenated nitrogen compounds to NO , whereas DC-8 uses CO , a compound not permitted on
 commercial aircraft (Bradshaw et al., 1998; Volz-Thomas et al., 2005; Thomas et al., 2015). The H_2 reagent
 converts anywhere from 2 to 20% of HCN to NO_y (Weinheimer, 2006). HCN ambient concentrations typically
 250 seasonally vary from ~200 to 300 pptv in the upper troposphere, amounting to an interference of 4-60 pptv (Li et
 al., 2003; Le Breton et al., 2013).

250

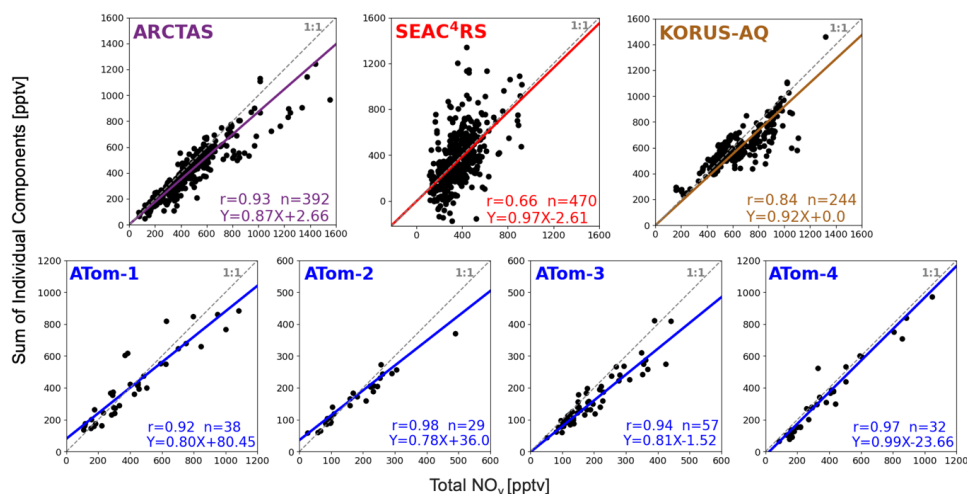


255 **Figure 3: Seasonality of northern hemisphere upper tropospheric NO_y .** Panels show seasonal means and medians (a) and seasonal transitions (b) of collocated gridded $2^\circ \times 2.5^\circ$ NO_y from IAGOS (orange), DC-8 (grey), and GEOS-Chem (red). Data in (a) are medians (lines), 25th and 75th percentiles (boxes) and means (diamonds). Inset text in (a) gives the number (n) of overlapping grid cells. Seasonality in (b) is the change in median NO_y in (a) from one season to the next.



260 Figure 4 shows the relationship between the sum of individual NO_y components and total NO_y for each DC-8 campaign. We use these scatterplots to determine whether most NO_y components are measured in each campaign, given our intention to use DC-8 to assess contemporary understanding of upper tropospheric NO_y. The individual components of NO_y summed to compare to total NO_y include NO; PSS NO₂ (Equation (1)); HNO₃; PAN measured as PAN for all ATom sub-campaigns and as part of total PNs for ARCTAS, SEAC⁴RS and KORUS-AQ; HNO₄ measured as HNO₄ for ATom-1 and -2 and as part of total PNs for ARCTAS, SEAC⁴RS and KORUS-AQ; C1-265 C5 ALKNs for all AToMs; total ALKNs for SEAC⁴RS, KORUS-AQ, and ARCTAS; PPN and other PANs for all except ATom-1 and -2; and MPN as part of total PNs for ARCTAS, SEAC⁴RS and KORUS-AQ. The evaluation in Figure 4 is biased toward the northern hemisphere, as the low time resolution sampling of ALKNs during ATom leads to loss of data in the southern hemisphere (Figure 2) to achieve coincidence of DC-8 total and individual components of NO_y.

270



275 **Figure 4: Proportion of reactive nitrogen components measured during each campaign. Individual points compare the coincident sum of individual NO_y components to measured total NO_y during NASA DC-8 campaigns. Individual NO_y components used in the figure are detailed in the text. Dashed grey lines are the 1:1 relationship. Coloured lines and inset equations are the Theil-Sen regression fit to the observations. Other inset values are the Pearson's correlation coefficient (r) and number of points (n). Axis ranges differ in each panel.**

280 Total measured NO_y and the sum of individual NO_y components are strongly correlated ($r > 0.8$) for all campaigns, except SEAC⁴RS ($r = 0.66$). The weaker correlation for SEAC⁴RS is from the large contribution of MPN to total PNs measured by the TD-LIF instrument. If instead we replace TD-LIF PNs with the sum of CIMS PANs and HNO₄, the correlation with total measured NO_y increases to $r = 0.91$, but the regression slope decreases from 0.97 in Figure 4 to 0.82, as MPN is ~20% of SEAC⁴RS NO_y. The large contribution of MPN to total NO_y during SEAC⁴RS is from aged air initially influenced by lightning, biomass burning and deep convective uplift of surface 285 pollution with large amounts of VOCs and NO_x. These large amounts of VOCs and NO_x cause very active photochemistry that enhances abundance of the MPN precursor, CH₃O₂ (Nault et al., 2015; Browne et al., 2011).



The regression slopes in Figure 4 indicate that most NO_y components are measured during each campaign, ranging from 0.78 for ATom-2 (78% of individual NO_y components measured) to 0.99 for ATom-4 (99% measured). The slopes suggest that between 1-22% of NO_y originates either from unmeasured components, positive interference in the NO_y instrument, or a combination of both. Bradshaw et al. (1998) estimated a temperature-dependent interference from HCN of 8-15% for chemiluminescence instruments that, like those deployed on DC-8 campaigns, use a CO reagent. We estimate a lower-end (8%) interference for mean ambient upper troposphere temperatures measured along the flight paths in Figure 2. Using DC-8 HCN observations, this amounts to ~ 53 ppt or 12% of NO_y for ARCTAS, ~ 19 pptv or 5% of NO_y for SEAC⁴RS, ~ 40 pptv or 6% NO_y for KORUS-AQ, and ~ 17 pptv or 6% of NO_y for ATom 1-4.

3.2 Upper tropospheric NO_y composition

Figure 5 provides a breakdown of the absolute and relative contributions of individual NO_y components to total NO_y . ATom-1 and -4 are combined, as these sub-campaigns have a very similar range in NO_y (Figure 4) and in median total and individual components of NO_y , as the sampled seasons (spring and summer) have very similar NO_y (Figure 3). Similarly, ATom-2 and -3 (autumn and winter) are combined. Campaigns are further grouped into remote (ARCTAS, ATom) and continental (SEAC⁴RS, KORUS-AQ), as local influence from continental sources like anthropogenic emissions and intense lightning leads to a greater relative contribution of NO_x and lesser contribution of PAN for the continental upper troposphere and vice versa for the remote upper troposphere.

305

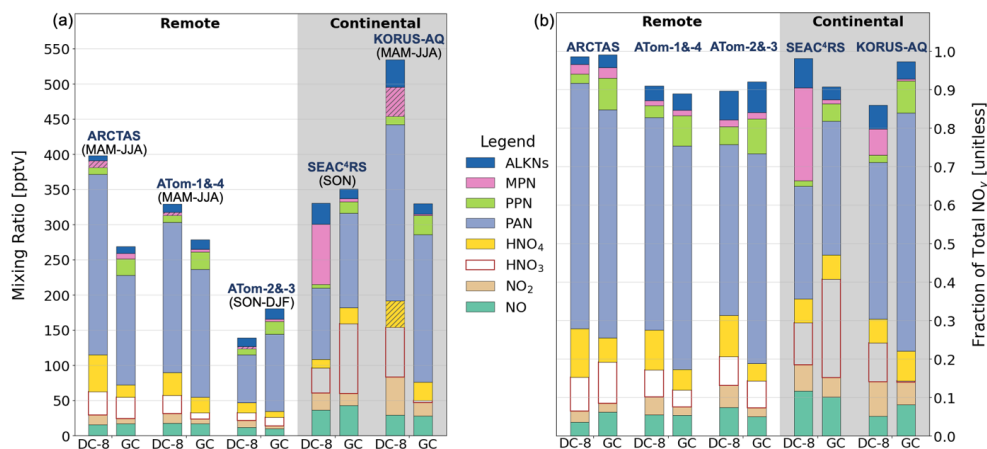


Figure 5: NO_y composition in the upper troposphere along DC-8 flight tracks. Bars are median values of absolute (a) and relative (b) individual NO_y components observed and inferred from the observations during DC-8 campaigns and simulated by GEOS-Chem (GC). Seasons sampled are given above each bar (a) and the grey shading distinguishes sampling in the remote (no shading) and continental (shaded) upper troposphere. Hatching in (a) indicate inferred concentrations (see text for details). Bar components from bottom to top are NO, NO_2 , HNO_3 , HNO_4 , PAN, PPN, MPN, and ALKNs.

DC-8 quantities in Figure 5 not directly measured are inferred. These include ATom-3 and -4 HNO_4 , ATom-1 and -2 PPN, ARCTAS MPN, KORUS-AQ HNO_4 and MPN, and ATom MPN. We use ATom-1 HNO_4 and ATom-



4 PPN for combined ATom-1 and -4 components, and, similarly, ATom-2 HNO₄ and ATom-3 PPN for combined ATom-2 and -3. ARCTAS upper tropospheric MPN of ~10 pptv is from the estimate by Browne et al. (2011). KORUS-AQ HNO₄ is estimated to be 37 pptv by multiplying the SEAC⁴RS median fraction of HNO₄ (HNO₄/NO_y = 0.06) by the KORUS-AQ median NO_y. SEAC⁴RS is used, as HNO₄ is thermally unstable (Ryerson et al., 2000) and so varies with temperature. Mean upper troposphere ambient temperatures for KORUS-AQ (252 K) are more consistent with SEAC⁴RS (246 K) than the other campaigns (238 K for ARCTAS, 238K-241 K for ATom).

KORUS-AQ MPN can be estimated by bounding a potential range from two approaches. The first is the median value of the difference between TD-LIF total PNs and the sum of all individual CIMs PANs and our inferred HNO₄, yielding MPN = 75 pptv. This likely overestimates MPN, as the CIMS instrument does not measure an exhaustive suite of PANs. Lee et al. (2022) estimated with a box model and KORUS-AQ measurements that unmeasured PANs account for ~20% of total PNs during KORUS-AQ, though this is for air masses impacted by petrochemical and other anthropogenic VOCs and NO_x emissions. Accounting for these unmeasured PANs yields a lower-bound KORUS-AQ MPN of 8 pptv. The MPN that we infer then for KORUS-AQ is 42 pptv, the midpoint of 8 and 75 pptv, accounting for 7% of KORUS-AQ NO_y. As the GEOS-Chem model MPN is consistent with DC-8 inferred MPN during ARCTAS, we multiply the GEOS-Chem ATom MPN fractions (MPN/NO_y ~0.01 for ATom-1 and -4 and ~0.02 for ATom-2 and -3) by ATom DC-8 NO_y to infer ATom MPN.

It is challenging to infer concentrations of longer chain (>C₅) ALKNs during ATom, so only the C₁-C₅ ALKNs are shown in Figure 5. The remote measurements of total ALKNs available from ARCTAS that would be most suitable to use to infer ATom total ALKNs are on median 5 pptv less than the ATom C₁-C₅ ALKNs measurements and are very noisy, as indicated by a range of -113 pptv to ~333 pptv. The range in ARCTAS WAS C₁-C₅ measurements, by comparison, is 8-29 pptv. Contributions of >C₅ ALKNs to total ALKNs for SEAC⁴RS (~50%) and KORUS-AQ (~60%), representative of the continental upper troposphere, can only be used to suggest that >C₅ ALKNs in remote regions are <50% of total ALKNs or <12 pptv (median of C₁-C₅ ALKNs for ATom1-4). According to the measurements, remote region C₁-C₅ ALKNs are dominated by methyl nitrate (C₁ ALKN), accounting for 40% of ATom C₁-C₅ ALKNs and 49% for ARCTAS. Second is isopropyl nitrate (C₃ ALKN), making up 17% of ATom C₁-C₅ ALKNs and 25% for ARCTAS. The >C₃ ALKNs dominate ALKNs in the continental upper troposphere, accounting for 92% of total ALKNs for SEAC⁴RS and 71% for KORUS-AQ. These we estimate as the difference between TD-LIF total ALKNs and the sum of WAS C₁-C₃ ALKNs.

The sum of KORUS-AQ NO_y components total 531 pptv, >130 pptv more than SEAC⁴RS, ARCTAS, and ATom-1 and -4 that are within a narrow range of 330-400 pptv. Minimum NO_y are for the remote autumn and winter measurements from ATom-2 and -3 at 141 pptv. Despite the wide range in absolute total and components of NO_y, the relative contribution of many individual NO_y components is consistent across all campaigns. These include NO (7 ± 3%; mean ± 1σ standard deviation), NO₂ (6 ± 2%), HNO₃ (9 ± 2%), HNO₄ (9 ± 3%), PPN (3 ± 1%), and ALKNs (5 ± 3%). PAN, the dominant NO_y component in all campaigns, is least consistent, ranging from 30-41% for the continental upper troposphere to 44-64% for the remote upper troposphere. The HNO₄ fraction (10-13%) in the remote upper troposphere is more than the continental upper troposphere (~6%), due to colder temperatures



for ATom and ARCTAS. MPN is uniquely prominent during SEAC⁴RS, accounting for 24% of NO_y compared to 2-7% inferred for all other campaigns.

360 The NO_y composition information in Figure 5 has a northern hemisphere sampling bias to achieve coincidence. ATom observations south of the Equator exhibit a similar seasonal pattern to the northern hemisphere: summer > spring > autumn > winter NO_y, except that the southern hemisphere spring and summer NO_y differ by ~90 pptv, whereas there is near-negligible difference for the northern hemisphere (Figure 3). As with the northern hemisphere, PAN accounts for most southern hemisphere NO_y, ranging from ~32% for ATom-1 (July-August) to ~42% for ATom-2 (January-February).

365 Measurements of the NO_y compounds nitrogen pentoxide (N₂O₅), the gas-phase nitrate radical (NO₃), and nitrous acid (HONO) are not included in Figure 5, as these are prominent at night and have near-negligible daytime abundances. Of these, there are only measurements of N₂O₅, limited to ATom-3 and -4, that represent ~0.1% of upper tropospheric NO_y along the daytime ATom flight tracks in Figure 2. NO₃ has a lifetime of a few seconds during the day, due to rapid photolysis and prompt reaction with NO (Brown and Stutz, 2012). HONO rapidly photolyzes with a near-surface lifetime of 15 min (Sörgel et al., 2011) that would be much shorter in the upper troposphere where photolysis frequencies are enhanced.

3.3 Contemporary understanding of UT NO_y

375 GEOS-Chem northern hemisphere upper troposphere NO_y is compared to the observations in Figures 3 and 5. In Figure 3, GEOS-Chem median NO_y is less than DC-8 in summer and spring by ~103 pptv, similar to DC-8 in autumn, and greater than DC-8 in winter by ~60 pptv. As a result of these differences in absolute NO_y, the model underestimates the IAGOS and DC-8 seasonal shifts in NO_y from winter to spring and from summer to autumn.

380 The sum of the GEOS-Chem fractional contributions of NO_y components in Figure 5(b) that do not sum to 1 are because the model NO_y budget also includes components not measured during DC-8, such as MPAN and halogenated ALKNs. Consistent across all campaigns is model underestimate in NO₂ and overestimate in PPN. The model version we use does not include photolysis of PPN, even though this is known to occur (Harwood et al., 2003). PPN photolysis rather than thermal decomposition is the dominant loss pathway of PPN in the cold upper troposphere. PPN photolysis is scheduled for inclusion in a later model version (version 14.5) than is used here (Horner et al., 2024). Inclusion of PPN photolysis would liberate up to ~16 pptv NO₂, resolving the 10-16 pptv model underestimate in NO₂. Other studies have addressed model biases in NO₂ by including photolysis of aerosol nitrate (pNO₃) forming HONO that rapidly photolyzes to NO_x (Shah et al., 2023; Horner et al., 2024).
385 pNO₃ concentrations are too small in the upper troposphere for this to be a substantial NO₂ source. Aerosol Mass Spectrometer (AMS) measurements of pNO₃ are on median ~0.01 μg m⁻³ during ARCTAS, ~0.07 μg m⁻³ during KOUS-AQ, ~0.04 μg m⁻³ during SEAC⁴RS and <0.01 μg m⁻³ during ATom.

390 The model exhibits significant campaign-specific biases in total NO_y for ARCTAS (129 pptv underestimate), KORUS-AQ (205 pptv underestimate), ATom-1 and -4 (51 pptv underestimate) and ATom-2 and -3 (42 pptv



overestimate). The model underestimate in ARCTAS NO_y is due mostly to a ~ 100 pptv low bias in PAN and, to a lesser extent, a 35 pptv underestimate in HNO_4 . The model bias for ATom-2 and -3 is due almost entirely to PAN. For KORUS-AQ, all NO_y components except PPN are underestimated, indicative of an overall underestimate in reactive nitrogen sources to the upper troposphere over this region. The ATom-1 and -4
400 underestimate in NO_y is due mostly to a low model bias in PAN and HNO_3 . Overall, the model underestimates the contrast in upper tropospheric NO_y between the remote and continental upper troposphere.

GEOS-Chem simulates individual C1-C3 ALKNs, but most $>C3$ ALKNs are included as a lumped species. There are other $>C3$ ALKNs represented individually in the model, such as those formed from isoprene oxidation (Fisher
405 et al., 2016), but abundances of these are near-negligible in the upper troposphere. DC-8 C1 ALKN is only 4% of ALKNs for SEAC⁴RS and 11% for KORUS-AQ, whereas in the model these are a much greater component of ALKNs: 40% for SEAC⁴RS and 29% for KORUS-AQ. Modelled $>C3$ ALKNs are a far smaller portion of total ALKNs (29% for SEAC⁴RS and 23% for KORUS-AQ) than the observations (Sect. 3.2). Modelled C1 ALKN concentrations are consistently less than the observed values by ~ 2 pptv for ARCTAS and ~ 1 pptv for ATom.
410 Modelled C3 ALKN is ~ 1 pptv less than the observations for ARCTAS, but ~ 1 pptv more than the observations for ATom.

The sum of measured and modelled individual NO_y components are not significantly different for SEAC⁴RS, though the model overestimates HNO_3 by 64 pptv and underestimates MPN by 81 pptv. The model low bias in
415 MPN suggests that the model underestimates influence of NO_x and reactive VOCs sources on aged air over source regions with a mix of emissions from fires and lightning, and deep convective injection of surface pollution. The model high bias in HNO_3 could be because of a factor of 2 model overestimate in H_2O_2 compared to observed H_2O_2 for SEAC⁴RS. An overestimate in H_2O_2 indicates a model overestimate in HO_2 that promotes formation of HNO_3 and that would also account for the ~ 10 pptv overestimate in modelled HNO_4 . Modelled HO_2 is used to
420 calculate PSS NO_2 for SEAC⁴RS (Equation (1), Sect. 2.1), but this only imparts a small high bias (~ 1.7 pptv) in SEAC⁴RS PSS NO_2 . Model bias in H_2O_2 for ARCTAS (>100 pptv) may also be the cause for the model underestimate in ARCTAS HNO_4 of ~ 35 pptv.

Modelled KORUS-AQ HNO_3 , ALKNs, and MPN are all biased low. The low biases in these NO_y components
425 may be because of a general underestimate in NO_y sources over South Korea where there are large anthropogenic NO_x and VOCs sources that are represented in the model with a global inventory (CEDs) that may not suitably account for local emissions (Travis et al., 2024). Lightning NO_x emissions could also be underestimated in the heavily parameterized inventory in GEOS-Chem (Murray et al., 2012; Marais et al., 2018), but this is a challenging
430 NO_x source to evaluate over locations that include other prominent sources of NO_x .

The model biases identified in this work hinder accurate determination of the radiative effect of tropospheric ozone for short-term climate impact assessments, the oxidative capacity of the troposphere for quantifying the lifetime and persistence of the greenhouse gas methane, tropospheric column densities of NO_2 from space-based UV-visible instruments that are retrieved with modelled vertical profiles of NO_2 , NO_x emissions by comparing



435 modelled and observed oxidized nitrate wet deposition fluxes that depend on the abundance of soluble HNO_3 , and
harm of reactive nitrogen deposition to vulnerable habitats.

4 Conclusions

440 We used NASA DC-8 aircraft measurement data from the ARCTAS, SEAC⁴RS, KORUS-AQ, and ATom
campaigns to characterize reactive nitrogen (NO_y) in the global upper troposphere. This followed confirmation
from comparison to routine reactive nitrogen measurements from the IAGOS commercial aircraft campaign that
DC-8 has the same seasonality of peak NO_y in summer and spring and minimum NO_y in winter in the northern
hemisphere. Consistency supports use of DC-8 campaign data to characterise NO_y under standard daytime
445 conditions.

We also confirm that most (78-99%) NO_y components were measured during DC-8 campaigns. These include
nitrogen oxides (NO_x), and inorganic (HNO_3 and HNO_4), and organic (PANs, MPN, and alkyl nitrates) reservoirs
of NO_x . PAN is the dominant NO_y component for all campaigns (30-64%), followed by NO_x (6-18%), HNO_4 (6-
450 13%) and HNO_3 (7-11%). The relative contribution of most other components is similar across all campaigns,
except for MPN that is ~24% of NO_y for SEAC⁴RS over the southeast US and much less (2-7%) for all other
campaigns, though the latter range is from inferred concentrations of MPN.

The GEOS-Chem model is sampled along the DC-8 flight tracks to assess the state of knowledge of upper
455 tropospheric NO_y . Consistent model biases for all campaigns include an overestimate in PPN and underestimate
in NO_2 . The model lacks PPN photolysis that would address the PPN model bias and mostly resolve the NO_2 bias.
In the continental upper troposphere, the model underestimates total NO_y for KORUS-AQ, but reproduces total
 NO_y for SEAC⁴RS, though with too much HNO_3 and too little MPN. Over remote regions, the model biases are
less severe, and are likely related to the weak seasonal variability in total NO_y in comparison to DC-8 and IAGOS.
460 A possible cause of this is errors in model representation of maritime lightning NO_x emissions that influence NO_y
abundance in spring and summer.

Our results underscore the need for sustained measurements of upper tropospheric reactive nitrogen for further
refinement of knowledge of upper tropospheric NO_y sources, advection, and chemical processing. This is crucial
465 for advancing our understanding of the global nitrogen cycle and its broader environmental implications.

Author Contributions

Study concept by EAM and NW. NW led the data analysis and simulated GEOS-Chem. The manuscript is initiated
by NW and co-written with EAM. GL aided in data analysis, RGR in the use of ObsPack, and BS in the use of
470 IAGOS NO_y observations. All authors reviewed and edited the manuscript.

Competing interests

The authors declare that they have no conflict of interest.



475 **Acknowledgements**

We are grateful for the provision of the NASA DC-8 aircraft observations provided by the instrument PIs Paul O. Wennberg, Ronald C. Cohen, Thomas B. Ryerson, Chelsea Thompson, Andrew Weinheimer, L. Gregory Huey, Jim Elkins, and Donald R. Blake and, for IAGOS, the IAGOS-Core data provided by Andreas Volz-Thomas and IAGOS-CARABIC by Helmut Ziereis. The authors acknowledge the strong support of the European Commission, Airbus, and the airlines (Lufthansa, Air France, Austrian Airlines, Air Namibia, Cathay Pacific, Iberia and China Airlines so far) who have carried the IAGOS-Core equipment and performed the maintenance since 1994. IAGOS-CARABIC NO_y measurement funding is from the German Aerospace Centre (DLR). In its last 10 years of operation, IAGOS-Core has been funded by INSU–CNRS (France), Météo-France, Université Paul Sabatier (Toulouse, France) and Forschungszentrum Jülich (FZJ, Jülich, Germany). IAGOS has been additionally funded by the EU projects IAGOSDS and IAGOS-ERI. The IAGOS-Core and the IAGOS-CARIBIC database are supported by AERIS. IAGOS-CARIBIC data are also available from the IAGOS-CARIBIC team (see <http://www.caribic-atmospheric.com>)

490 **Data and Software Availability**

All data and software used in this study are from publicly accessible repositories cited in the text.

Funding

This research has been supported by the European Research Council under the European Union's Horizon 2020 research and innovation programme (through a Starting Grant awarded to Eloise A. Marais, UpTrop [grant no. 851854]).

References

- Amos, H. M., Jacob, D. J., Holmes, C., Fisher, J. A., Wang, Q., Yantosca, R. M., Corbitt, E. S., Galarneau, E., Rutter, A., and Gustin, M.: Gas-particle partitioning of atmospheric Hg (II) and its effect on global mercury deposition, *Atmos. Chem. Phys.*, 12, 591-603, 2012.
- Barth, M. C., Cantrell, C. A., Brune, W. H., Rutledge, S. A., Crawford, J. H., Huntrieser, H., Carey, L. D., MacGorman, D., Weisman, M., Pickering, K. E., Bruning, E., Anderson, B., Apel, E., Biggstaff, M., Campos, T., Campuzano-Jost, P., Cohen, R., Crouse, J., Day, D. A., Diskin, G., Flocke, F., Fried, A., Garland, C., Heikes, B., Honomichl, S., Hornbrook, R., Huey, L. G., Jimenez, J. L., Lang, T., Lichtenstern, M., Mikoviny, T., Nault, B., O'Sullivan, D., Pan, L. L., Peischl, J., Pollack, I., Richter, D., Riemer, D., Ryerson, T., Schlager, H., St. Clair, J., Walega, J., Weibring, P., Weinheimer, A., Wennberg, P., Wisthaler, A., Wooldridge, P. J., and Ziegler, C.: The Deep Convective Clouds and Chemistry (DC3) Field Campaign, *B. Am. Meteorol. Soc.*, 96, 1281-1309, 10.1175/bams-d-13-00290.1, 2015.
- Bertram, T. H., Perring, A. E., Wooldridge, P. J., Crouse, J. D., Kwan, A. J., Wennberg, P. O., Scheuer, E., Dibb, J., Avery, M., Sachse, G., Vay, S. A., Crawford, J. H., McNaughton, C. S., Clarke, A., Pickering, K. E., Fuelberg, H., Huey, G., Blake, D. R., Singh, H. B., Hall, S. R., Shetter, R. E., Fried, A., Heikes, B. G., and Cohen, R. C.: Direct Measurements of the Convective Recycling of the Upper Troposphere, *Science*, 315, 816-820, doi:10.1126/science.1134548, 2007.
- Blake, N. J., Blake, D. R., Swanson, A. L., Atlas, E., Flocke, F., and Rowland, F. S.: Latitudinal, vertical, and seasonal variations of C1-C4 alkyl nitrates in the troposphere over the Pacific Ocean during PEM-Tropics A and B: Oceanic and continental sources, *J. Geophys. Res.-Atmos.*, 108, <https://doi.org/10.1029/2001JD001444>, 2003.



- Blakeslee, R. J., Mach, D. M., Bateman, M. G., and Bailey, J. C.: Seasonal variations in the lightning diurnal cycle and implications for the global electric circuit, *Atmos. Res.*, 135-136, 228-243, 520 <https://doi.org/10.1016/j.atmosres.2012.09.023>, 2014.
- Boersma, K. F., Eskes, H. J., Dirksen, R. J., van der A, R. J., Veeckind, J. P., Stammes, P., Huijnen, V., Kleipool, Q. L., Sneep, M., Claas, J., Leitão, J., Richter, A., Zhou, Y., and Brunner, D.: An improved tropospheric NO₂ column retrieval algorithm for the Ozone Monitoring Instrument, *Atmos. Meas. Tech.*, 4, 1905-1928, 10.5194/amt-4-1905-2011, 2011.
- Bourgeois, I., Peischl, J., Neuman, J. A., Brown, S. S., Allen, H. M., Campuzano-Jost, P., Coggon, M. M., DiGangi, J. P., Diskin, G. S., Gilman, J. B., Gkatzelis, G. I., Guo, H., Halliday, H. A., Hanco, T. F., Holmes, C. D., Huey, L. G., Jimenez, J. L., Lamplugh, A. D., Lee, Y. R., Lindaas, J., Moore, R. H., Nault, B. A., Nowak, J. B., Pagonis, D., Rickly, P. S., Robinson, M. A., Rollins, A. W., Selimovic, V., St. Clair, J. M., Tanner, D., Vasquez, K. T., Veres, P. R., Warneke, C., Wennberg, P. O., Washenfelder, R. A., Wiggins, E. B., Womack, C. C., Xu, L., Zarzana, K. J., and Ryerson, T. B.: Comparison of airborne measurements of NO, NO₂, HONO, 530 NO_y, and CO during FIREX-AQ, *Atmos. Meas. Tech.*, 15, 4901-4930, 10.5194/amt-15-4901-2022, 2022.
- Bradshaw, J., Sandholm, S., and Talbot, R.: An update on reactive odd-nitrogen measurements made during recent NASA Global Tropospheric Experiment programs, *J. Geophys. Res.-Atmos.*, 103, 19129-19148, <https://doi.org/10.1029/98JD00621>, 1998.
- Bradshaw, J., Davis, D., Grodzinsky, G., Smyth, S., Newell, R., Sandholm, S., and Liu, S.: Observed distributions of nitrogen oxides in the remote free troposphere from the Nasa Global Tropospheric Experiment Programs, *Rev. Geophys.*, 38, 61-116, 10.1029/1999rg900015, 2000.
- Brasseur, G. P., Müller, J.-F., and Granier, C.: Atmospheric impact of NO_x emissions by subsonic aircraft: A three dimensional model study, *J. Geophys. Res.-Atmos.*, 101, 1423-1428, 10.1029/95jd02363, 1996.
- Brenninkmeijer, C. A. M., Crutzen, P., Boumard, F., Dauer, T., Dix, B., Ebinghaus, R., Filippi, D., Fischer, H., Franke, H., Frieß, U., Heintzenberg, J., Helleis, F., Hermann, M., Kock, H. H., Koepfel, C., Lelieveld, J., Leuenberger, M., Martinsson, B. G., Miemczyk, S., Moret, H. P., Nguyen, H. N., Nyfeler, P., Oram, D., O'Sullivan, D., Penkett, S., Platt, U., Pucek, M., Ramonet, M., Randa, B., Reichelt, M., Rhee, T. S., Rohwer, J., Rosenfeld, K., Scharffe, D., Schlager, H., Schumann, U., Slemr, F., Sprung, D., Stock, P., Thaler, R., Valentino, F., van Velthoven, P., Waibel, A., Wandel, A., Waschitschek, K., Wiedensohler, A., Xueref-Remy, I., Zahn, A., Zech, U., and Ziereis, H.: Civil Aircraft for the regular investigation of the atmosphere based on an instrumented container: The new CARIBIC system, *Atmos. Chem. Phys.*, 7, 4953-4976, 10.5194/acp-7-4953-2007, 2007.
- Brown, S. S. and Stutz, J.: Nighttime radical observations and chemistry, *Chem. Soc. Rev.*, 41, 6405-6447, 10.1039/C2CS35181A, 2012.
- Browne, E. C., Perring, A. E., Wooldridge, P. J., Apel, E., Hall, S. R., Huey, L. G., Mao, J., Spencer, K. M., Clair, J. M. S., Weinheimer, A. J., Wisthaler, A., and Cohen, R. C.: Global and regional effects of the photochemistry of CH₃O₂NO₂: evidence from ARCTAS, *Atmos. Chem. Phys.*, 11, 4209-4219, 10.5194/acp-11-4209-2011, 2011.
- Burkholder, J. B., Sander, S. P., Abbatt, J., Barker, J. R., Cappa, C., Crouse, J. D., Dibble, T. S., Huie, R. E., Kolb, C. E., Kurylo, M. J., Orkin, V. L., Percival, C. J., Wilmouth, D. M., and Wine, P. H.: Chemical kinetics and photochemical data for use in atmospheric studies, evaluation No. 19, JPL Publication 19-5, <https://jpldataeval.jpl.nasa.gov/pdf/NASA-JPL%20Evaluation%2019-5.pdf> (last access: 24 October 2024), 2020.
- Cohen, Y., Hauglustaine, D., Sauvage, B., Rohs, S., Konjari, P., Bundke, U., Petzold, A., Thouret, V., Zahn, A., and Ziereis, H.: Evaluation of modelled climatologies of O₃, CO, water vapour and NO_y in the upper troposphere–lower stratosphere using regular in situ observations by passenger aircraft, *Atmos. Chem. Phys.*, 23, 14973-15009, 10.5194/acp-23-14973-2023, 2023.



- 565 Crawford, J. H., Ahn, J.-Y., Al-Saadi, J., Chang, L., Emmons, L. K., Kim, J., Lee, G., Park, J.-H., Park, R. J., Woo, J. H., Song, C.-K., Hong, J.-H., Hong, Y.-D., Lefter, B. L., Lee, M., Lee, T., Kim, S., Min, K.-E., Yum, S. S., Shin, H. J., Kim, Y.-W., Choi, J.-S., Park, J.-S., Szykman, J. J., Long, R. W., Jordan, C. E., Simpson, I. J., Fried, A., Dibb, J. E., Cho, S., and Kim, Y. P.: The Korea–United States Air Quality (KORUS-AQ) field study, *Elementa: Science of the Anthropocene*, 9, 10.1525/elementa.2020.00163, 2021.
- 570 Crouse, J. D., McKinney, K. A., Kwan, A. J., and Wennberg, P. O.: Measurement of Gas-Phase Hydroperoxides by Chemical Ionization Mass Spectrometry, *Anal. Chem.*, 78, 6726-6732, 10.1021/ac0604235, 2006.
- Culter, F.: NASA DC-8 Flying Laboratory Aircraft, 2009.
- Dahlmann, K., Grewe, V., Ponater, M., and Matthes, S.: Quantifying the contributions of individual NO_x sources to the trend in ozone radiative forcing, *Atmos. Environ.*, 45, 2860-2868, 10.1016/j.atmosenv.2011.02.071, 2011.
- 575 Dameris, M.: Stratosphere/Troposphere exchange and structure | Tropopause, in: *Encyclopedia of Atmospheric Sciences (Second Edition)*, edited by: North, G. R., Pyle, J., and Zhang, F., Academic Press, Oxford, 269-272, <https://doi.org/10.1016/B978-0-12-382225-3.00418-7>, 2015.
- Ehhalt, D. H., Rohrer, F., and Wahner, A.: Sources and distribution of NO_x in the upper troposphere at northern mid-latitudes, *J. Geophys. Res.-Atmos.*, 97, 3725-3738, <https://doi.org/10.1029/91JD03081>, 1992.
- 580 Fisher, J. A., Atlas, E. L., Barletta, B., Meinardi, S., Blake, D. R., Thompson, C. R., Ryerson, T. B., Peischl, J., Tzompa-Sosa, Z. A., and Murray, L. T.: Methyl, Ethyl, and Propyl Nitrates: Global Distribution and Impacts on Reactive Nitrogen in Remote Marine Environments, *J. Geophys. Res.-Atmos.*, 123, 10.1029/2018jd029046, 2018.
- 585 Fisher, J. A., Jacob, D. J., Travis, K. R., Kim, P. S., Marais, E. A., Chan Miller, C., Yu, K., Zhu, L., Yantosca, R. M., Sulprizio, M. P., Mao, J., Wennberg, P. O., Crouse, J. D., Teng, A. P., Nguyen, T. B., St. Clair, J. M., Cohen, R. C., Romer, P., Nault, B. A., Wooldridge, P. J., Jimenez, J. L., Campuzano-Jost, P., Day, D. A., Hu, W., Shepson, P. B., Xiong, F., Blake, D. R., Goldstein, A. H., Misztal, P. K., Hanisco, T. F., Wolfe, G. M., Ryerson, T. B., Wisthaler, A., and Mikoviny, T.: Organic nitrate chemistry and its implications for nitrogen budgets in an isoprene- and monoterpene-rich atmosphere: constraints from aircraft (SEAC4RS) and ground-based (SOAS) observations in the Southeast US, *Atmos. Chem. Phys.*, 16, 5969-5991, 10.5194/acp-16-5969-2016, 2016.
- 590 Fuelberg, H. E., Hannan, J. R., van Velthoven, P. F. J., Browell, E. V., Bieberbach Jr., G., Knabb, R. D., Gregory, G. L., Pickering, K. E., and Selkirk, H. B.: A meteorological overview of the Subsonic Assessment Ozone and Nitrogen Oxide Experiment (SONEX) period, *J. Geophys. Res.-Atmos.*, 105, 3633-3651, <https://doi.org/10.1029/1999JD900917>, 2000.
- Giglio, L., Randerson, J. T., and van der Werf, G. R.: Analysis of daily, monthly, and annual burned area using the fourth-generation global fire emissions database (GFED4), *J. Geophys. Res.-Biogeo.*, 118, 317-328, <https://doi.org/10.1002/jgrg.20042>, 2013.
- 600 Gressent, A., Sauvage, B., Cariolle, D., Evans, M., Leriche, M., Mari, C., and Thouret, V.: Modeling lightning-NO_x chemistry on a sub-grid scale in a global chemical transport model, *Atmos. Chem. Phys.*, 16, 5867-5889, 10.5194/acp-16-5867-2016, 2016.
- Gressent, A., Sauvage, B., Defer, E., Pätz, H. W., Thomas, K., Holle, R., Cammas, J.-P., Nédélec, P., Boulanger, D., Thouret, V., and Volz-Thomas, A.: Lightning NO_x influence on large-scale NO_y and O₃ plumes observed over the northern mid-latitudes, *Tellus B*, 66, 10.3402/tellusb.v66.25544, 2014.



- 605 Guenther, A. B., Jiang, X., Heald, C. L., Sakulyanontvittaya, T., Duhl, T., Emmons, L. K., and Wang, X.: The Model of Emissions of Gases and Aerosols from Nature version 2.1 (MEGAN2.1): an extended and updated framework for modeling biogenic emissions, *Geosci. Model Dev.*, 5, 1471-1492, 10.5194/gmd-5-1471-2012, 2012.
- 610 Harwood, M. H., Roberts, J. M., Frost, G. J., Ravishankara, A. R., and Burkholder, J. B.: Photochemical Studies of $\text{CH}_3\text{C}(\text{O})\text{OONO}_2$ (PAN) and $\text{CH}_3\text{CH}_2\text{C}(\text{O})\text{OONO}_2$ (PPN): NO_3 Quantum Yields, *J. Phys. Chem. A*, 107, 1148-1154, 10.1021/jp0264230, 2003.
- 615 Hoesly, R. M., Smith, S. J., Feng, L., Klimont, Z., Janssens-Maenhout, G., Pitkanen, T., Seibert, J. J., Vu, L., Andres, R. J., Bolt, R. M., Bond, T. C., Dawidowski, L., Kholod, N., Kurokawa, J. I., Li, M., Liu, L., Lu, Z., Moura, M. C. P., O'Rourke, P. R., and Zhang, Q.: Historical (1750–2014) anthropogenic emissions of reactive gases and aerosols from the Community Emissions Data System (CEDS), *Geosci. Model Dev.*, 11, 369-408, 10.5194/gmd-11-369-2018, 2018.
- Horner, R. P., Marais, E. A., Wei, N., Ryan, R. G., and Shah, V.: Vertical profiles of global tropospheric nitrogen dioxide (NO_2) obtained by cloud-slicing TROPOMI, *Atmos. Chem. Phys.*, 2024, 1-29, 10.5194/egusphere-2024-1541, 2024.
- 620 Hudman, R. C., Moore, N. E., Mebust, A. K., Martin, R. V., Russell, A. R., Valin, L. C., and Cohen, R. C.: Steps towards a mechanistic model of global soil nitric oxide emissions: implementation and space based-constraints, *Atmos. Chem. Phys.*, 12, 7779-7795, 10.5194/acp-12-7779-2012, 2012.
- 625 Hudman, R. C., Jacob, D. J., Turquety, S., Leibensperger, E. M., Murray, L. T., Wu, S., Gilliland, A. B., Avery, M., Bertram, T. H., Brune, W., Cohen, R. C., Dibb, J. E., Flocke, F. M., Fried, A., Holloway, J., Neuman, J. A., Orville, R., Perring, A., Ren, X., Sachse, G. W., Singh, H. B., Swanson, A., and Wooldridge, P. J.: Surface and lightning sources of nitrogen oxides over the United States: Magnitudes, chemical evolution, and outflow, *J. Geophys. Res.*, 112, 10.1029/2006jd007912, 2007.
- 630 Huntrieser, H., Lichtenstern, M., Scheibe, M., Aufmhoff, H., Schlager, H., Pucik, T., Minikin, A., Weinzierl, B., Heimerl, K., Pollack, I. B., Peischl, J., Ryerson, T. B., Weinheimer, A. J., Honomichl, S., Ridley, B. A., Biggerstaff, M. I., Betten, D. P., Hair, J. W., Butler, C. F., Schwartz, M. J., and Barth, M. C.: Injection of lightning-produced NO_x , water vapor, wildfire emissions, and stratospheric air to the UT/LS as observed from DC3 measurements, *J. Geophys. Res.-Atmos.*, 121, 6638-6668, <https://doi.org/10.1002/2015JD024273>, 2016.
- 635 Jacob, D. J., Crawford, J. H., Maring, H., Clarke, A. D., Dibb, J. E., Emmons, L. K., Ferrare, R. A., Hostetler, C. A., Russell, P. B., Singh, H. B., Thompson, A. M., Shaw, G. E., McCauley, E., Pederson, J. R., and Fisher, J. A.: The Arctic Research of the Composition of the Troposphere from Aircraft and Satellites (ARCTAS) mission: design, execution, and first results, *Atmos. Chem. Phys.*, 10, 5191-5212, 10.5194/acp-10-5191-2010, 2010.
- 640 Jaeglé, L., Jacob, D. J., Wang, Y., Weinheimer, A. J., Ridley, B. A., Campos, T. L., Sachse, G. W., and Hagen, D. E.: Sources and chemistry of NO_x in the upper troposphere over the United States, *Geophys. Res. Lett.*, 25, 1705-1708, 10.1029/97gl03591, 1998.
- 645 Le Breton, M., Bacak, A., Muller, J. B. A., O'Shea, S. J., Xiao, P., Ashfold, M. N. R., Cooke, M. C., Batt, R., Shallcross, D. E., Oram, D. E., Forster, G., Bauguitte, S. J. B., Palmer, P. I., Parrington, M., Lewis, A. C., Lee, J. D., and Percival, C. J.: Airborne hydrogen cyanide measurements using a chemical ionisation mass spectrometer for the plume identification of biomass burning forest fires, *Atmos. Chem. Phys.*, 13, 9217-9232, 10.5194/acp-13-9217-2013, 2013.
- Lee, Y. R., Huey, L. G., Tanner, D. J., Takeuchi, M., Qu, H., Liu, X., Ng, N. L., Crawford, J. H., Fried, A., Richter, D., Simpson, I. J., Blake, D. R., Blake, N. J., Meinardi, S., Kim, S., Diskin, G. S., Digangi, J. P., Choi, Y., Pusede, S. E., Wennberg, P. O., Kim, M. J., Crounse, J. D., Teng, A. P., Cohen, R. C., Romer, P. S., Brune, W., Wisthaler, A., Mikoviny, T., Jimenez, J. L., Campuzano-Jost, P., Nault, B. A., Weinheimer, A., Hall, S. R.,



- 650 and Ullmann, K.: An investigation of petrochemical emissions during KORUS-AQ: Ozone production, reactive nitrogen evolution, and aerosol production, *Elementa: Science of the Anthropocene*, 10, 10.1525/elementa.2022.00079, 2022.
- Levy II, H., Mahlman, J. D., and Moxim, W. J.: A stratospheric source of reactive nitrogen in the unpolluted troposphere, *Geophys. Res. Lett.*, 7, 441-444, <https://doi.org/10.1029/GL007i006p00441>, 1980.
- 655 Levy II, H., Moxim, W. J., Klonecki, A. A., and Kasibhatla, P. S.: Simulated tropospheric NO_x: Its evaluation, global distribution and individual source contributions, *J. Geophys. Res.-Atmos.*, 104, 26279-26306, <https://doi.org/10.1029/1999JD900442>, 1999.
- Li, Q., Jacob, D. J., Yantosca, R. M., Heald, C. L., Singh, H. B., Koike, M., Zhao, Y., Sachse, G. W., and Streets, D. G.: A global three-dimensional model analysis of the atmospheric budgets of HCN and CH₃CN: Constraints from aircraft and ground measurements, *J. Geophys. Res.-Atmos.*, 108, <https://doi.org/10.1029/2002JD003075>, 2003.
- 660 Liang, Q., Rodriguez, J. M., Douglass, A. R., Crawford, J. H., Olson, J. R., Apel, E., Bian, H., Blake, D. R., Brune, W., Chin, M., Colarco, P. R., da Silva, A., Diskin, G. S., Duncan, B. N., Huey, L. G., Knapp, D. J., Montzka, D. D., Nielsen, J. E., Pawson, S., Riemer, D. D., Weinheimer, A. J., and Wisthaler, A.: Reactive nitrogen, ozone and ozone production in the Arctic troposphere and the impact of stratosphere-troposphere exchange, *Atmos. Chem. Phys.*, 11, 13181-13199, 10.5194/acp-11-13181-2011, 2011.
- 665 Logan, J. A.: Nitrogen oxides in the troposphere: Global and regional budgets, *J. Geophys. Res.-Oceans*, 88, 10785-10807, <https://doi.org/10.1029/JC088iC15p10785>, 1983.
- Luo, G., Yu, F., and Moch, J. M.: Further improvement of wet process treatments in GEOS-Chem v12.6.0: impact on global distributions of aerosols and aerosol precursors, *Geosci. Model Dev.*, 13, 2879-2903, 10.5194/gmd-13-2879-2020, 2020.
- 670 Marais, E. A., Jacob, D. J., Choi, S., Joiner, J., Belmonte-Rivas, M., Cohen, R. C., Beirle, S., Murray, L. T., Schiferl, L. D., Shah, V., and Jaeglé, L.: Nitrogen oxides in the global upper troposphere: interpreting cloud-sliced NO₂ observations from the OMI satellite instrument, *Atmos. Chem. Phys.*, 18, 17017-17027, 10.5194/acp-18-17017-2018, 2018.
- 675 Marais, E. A., Roberts, J. F., Ryan, R. G., Eskes, H., Boersma, K. F., Choi, S., Joiner, J., Abuhassan, N., Redondas, A., Grutter, M., Cede, A., Gomez, L., and Navarro-Comas, M.: New observations of NO₂ in the upper troposphere from TROPOMI, *Atmos. Meas. Tech.*, 14, 2389-2408, 10.5194/amt-14-2389-2021, 2021.
- Marengo, A., Thouret, V., Nédélec, P., Smit, H., Helten, M., Kley, D., Karcher, F., Simon, P., Law, K., Pyle, J., Poschmann, G., Von Wrede, R., Hume, C., and Cook, T.: Measurement of ozone and water vapor by Airbus in-service aircraft: The MOZAIC airborne program, an overview, *J. Geophys. Res.-Atmos.*, 103, 25631-25642, 10.1029/98jd00977, 1998.
- 680 Mickley, L. J., Murti, P. P., Jacob, D. J., Logan, J. A., Koch, D. M., and Rind, D.: Radiative forcing from tropospheric ozone calculated with a unified chemistry-climate model, *J. Geophys. Res.-Atmos.*, 104, 30153-30172, 10.1029/1999jd900439, 1999.
- 685 Murray, L. T., Logan, J. A., and Jacob, D. J.: Interannual variability in tropical tropospheric ozone and OH: The role of lightning, *J. Geophys. Res.-Atmos.*, 118, 4114-4118, 10.1029/2013JD019857, 2013.
- Murray, L. T., Fiore, A. M., Shindell, D. T., Naik, V., and Horowitz, L. W.: Large uncertainties in global hydroxyl projections tied to fate of reactive nitrogen and carbon, *P. Natl. Acad. Sci. USA*, 118, e2115204118, doi:10.1073/pnas.2115204118, 2021.
- 690



Murray, L. T., Jacob, D. J., Logan, J. A., Hudman, R. C., and Koshak, W. J.: Optimized regional and interannual variability of lightning in a global chemical transport model constrained by LIS/OTD satellite data, *J. Geophys. Res.-Atmos.*, 117, 10.1029/2012jd017934, 2012.

695 NASA: Airborne Science Data for Atmospheric Composition: <https://www-air.larc.nasa.gov/cgi-bin/ArcView/arctas?DC8=1>, (last access: 24 October).

NASA: Airborne Science Data for Atmospheric Composition: <https://www-air.larc.nasa.gov/cgi-bin/ArcView/seac4rs>, (last access: 24 October).

NASA: EARTHDATA, Korea United States Air Quality Study: <https://asdc.larc.nasa.gov/project/KORUS-AQ>, (last access: 24 October).

700 NASA: EARTHDATA, ATom: Merged Atmospheric Chemistry, Trace Gases, and Aerosols, Version 2: https://daac.ornl.gov/cgi-bin/dsviewer.pl?ds_id=1925, (last access: 24 October).

Nault, B. A., Garland, C., Pusede, S. E., Wooldridge, P. J., Ullmann, K., Hall, S. R., and Cohen, R. C.: Measurements of CH₃O₂NO₂ in the upper troposphere, *Atmos. Meas. Tech.*, 8, 987-997, 10.5194/amt-8-987-2015, 2015.

705 Petzold, A., Thouret, V., Gerbig, C., Zahn, A., Brenninkmeijer, C. A. M., Gallagher, M., Hermann, M., Pontaud, M., Ziereis, H., Boulanger, D., Marshall, J., Nédélec, P., Smit, H. G. J., Friess, U., Flaud, J.-M., Wahner, A., Cammas, J.-P., and Volz-Thomas, A.: Global-scale atmosphere monitoring by in-service aircraft – current achievements and future prospects of the European Research Infrastructure IAGOS, *Tellus B*, 67, 28452, 10.3402/tellusb.v67.28452, 2015.

710 Pollack, I. B., Lerner, B. M., and Ryerson, T. B.: Evaluation of ultraviolet light-emitting diodes for detection of atmospheric NO₂ by photolysis - chemiluminescence, *J. Atmos. Chem.*, 65, 111-125, 10.1007/s10874-011-9184-3, 2010.

715 Prather, M. J. and Jacob, D. J.: A persistent imbalance in HO_x and NO_x photochemistry of the upper troposphere driven by deep tropical convection, *Geophys. Res. Lett.*, 24, 3189-3192, <https://doi.org/10.1029/97GL03027>, 1997.

Rap, A., Richards, N. A. D., Forster, P. M., Monks, S. A., Arnold, S. R., and Chipperfield, M. P.: Satellite constraint on the tropospheric ozone radiative effect, *Geophys. Res. Lett.*, 42, 5074-5081, 10.1002/2015gl064037, 2015.

720 Reed, C., Evans, M. J., Di Carlo, P., Lee, J. D., and Carpenter, L. J.: Interferences in photolytic NO₂ measurements: explanation for an apparent missing oxidant?, *Atmos. Chem. Phys.*, 16, 4707-4724, 10.5194/acp-16-4707-2016, 2016.

Roberts, J. M.: The atmospheric chemistry of organic nitrates, *Atmos. Environ. A-Gen.*, 24, 243-287, [https://doi.org/10.1016/0960-1686\(90\)90108-Y](https://doi.org/10.1016/0960-1686(90)90108-Y), 1990.

725 Roberts, J. M., Flocke, F., Stroud, C. A., Hereid, D., Williams, E., Fehsenfeld, F., Brune, W., Martinez, M., and Harder, H.: Ground-based measurements of peroxy-carboxylic nitric anhydrides (PANs) during the 1999 Southern Oxidants Study Nashville Intensive, *J. Geophys. Res.-Atmos.*, 107, ACH 1-1-ACH 1-10, <https://doi.org/10.1029/2001JD000947>, 2002.

730 Roberts, J. M., Williams, J., Baumann, K., Buhr, M. P., Goldan, P. D., Holloway, J., Hübler, G., Kuster, W. C., McKeen, S. A., Ryerson, T. B., Trainer, M., Williams, E. J., Fehsenfeld, F. C., Bertman, S. B., Nouaime, G., Seaver, C., Grodzinsky, G., Rodgers, M., and Young, V. L.: Measurements of PAN, PPN, and MPAN made



during the 1994 and 1995 Nashville Intensives of the Southern Oxidant Study: Implications for regional ozone production from biogenic hydrocarbons, *J. Geophys. Res.-Atmos.*, 103, 22473-22490, <https://doi.org/10.1029/98JD01637>, 1998.

- 735 Ryerson, T. B., Williams, E. J., and Fehsenfeld, F. C.: An efficient photolysis system for fast-response NO₂ measurements, *J. Geophys. Res.-Atmos.*, 105, 26447-26461, <https://doi.org/10.1029/2000JD900389>, 2000.
- Seltzer, K. M., Vizuete, W., and Henderson, B. H.: Evaluation of updated nitric acid chemistry on ozone precursors and radiative effects, *Atmos. Chem. Phys.*, 15, 5973-5986, 10.5194/acp-15-5973-2015, 2015.
- 740 Shah, V., Jacob, D. J., Dang, R., Lamsal, L. N., Strode, S. A., Steenrod, S. D., Boersma, K. F., Eastham, S. D., Fritz, T. M., Thompson, C., Peischl, J., Bourgeois, I., Pollack, I. B., Nault, B. A., Cohen, R. C., Campuzano-Jost, P., Jimenez, J. L., Andersen, S. T., Carpenter, L. J., Sherwen, T., and Evans, M. J.: Nitrogen oxides in the free troposphere: implications for tropospheric oxidants and the interpretation of satellite NO₂ measurements, *Atmos. Chem. Phys.*, 23, 1227-1257, 10.5194/acp-23-1227-2023, 2023.
- 745 Silvern, R. F., Jacob, D. J., Travis, K. R., Sherwen, T., Evans, M. J., Cohen, R. C., Laughner, J. L., Hall, S. R., Ullmann, K., Crounse, J. D., Wennberg, P. O., Peischl, J., and Pollack, I. B.: Observed NO/NO₂ Ratios in the Upper Troposphere Imply Errors in NO-NO₂-O₃ Cycling Kinetics or an Unaccounted NO_x Reservoir, *Geophys. Res. Lett.*, 45, 4466-4474, 10.1029/2018gl077728, 2018.
- Singh, H. B.: Reactive nitrogen in the troposphere, *Environ. Sci. Technol.*, 21, 320-327, 10.1021/es00158a001, 1987.
- 750 Singh, H. B., Thompson, A. M., and Schlager, H.: SONEX airborne mission and coordinated POLINAT-2 activity: Overview and accomplishments, *Geophys. Res. Lett.*, 26, 3053-3056, <https://doi.org/10.1029/1999GL900588>, 1999.
- Singh, H. B., Brune, W. H., Crawford, J. H., Flocke, F., and Jacob, D. J.: Chemistry and transport of pollution over the Gulf of Mexico and the Pacific: spring 2006 INTEX-B campaign overview and first results, *Atmos. Chem. Phys.*, 9, 2301-2318, 10.5194/acp-9-2301-2009, 2009.
- 755 Singh, H. B., Brune, W. H., Crawford, J. H., Jacob, D. J., and Russell, P. B.: Overview of the summer 2004 Intercontinental Chemical Transport Experiment–North America (INTEX-A), *J. Geophys. Res.-Atmos.*, 111, <https://doi.org/10.1029/2006JD007905>, 2006.
- 760 Slusher, D. L., Huey, L. G., Tanner, D. J., Flocke, F. M., and Roberts, J. M.: A thermal dissociation–chemical ionization mass spectrometry (TD-CIMS) technique for the simultaneous measurement of peroxyacyl nitrates and dinitrogen pentoxide, *J. Geophys. Res.-Atmos.*, 109, <https://doi.org/10.1029/2004JD004670>, 2004.
- Sörgel, M., Regelin, E., Bozem, H., Diesch, J. M., Drewnick, F., Fischer, H., Harder, H., Held, A., Hosaynali-Beygi, Z., Martinez, M., and Zetzsch, C.: Quantification of the unknown HONO daytime source and its relation to NO₂, *Atmos. Chem. Phys.*, 11, 10433-10447, 10.5194/acp-11-10433-2011, 2011.
- 765 Stettler, M. E. J., Eastham, S., and Barrett, S. R. H.: Air quality and public health impacts of UK airports. Part I: Emissions, *Atmos. Environ.*, 45, 5415-5424, 10.1016/j.atmosenv.2011.07.012, 2011.
- Stratmann, G., Ziereis, H., Stock, P., Brenninkmeijer, C. A. M., Zahn, A., Rauthe-Schöch, A., Velthoven, P. V., Schlager, H., and Volz-Thomas, A.: NO and NO_y in the upper troposphere: Nine years of CARIBIC measurements onboard a passenger aircraft, *Atmos. Environ.*, 133, 93-111, <https://doi.org/10.1016/j.atmosenv.2016.02.035>, 2016.



- 770 Talbot, R. W., Dibb, J. E., Scheuer, E. M., Kondo, Y., Koike, M., Singh, H. B., Salas, L. B., Fukui, Y., Ballenthin, J. O., Meads, R. F., Miller, T. M., Hutton, D. E., Viggiano, A. A., Blake, D. R., Blake, N. J., Atlas, E., Flocke, F., Jacob, D. J., and Jaegle, L.: Reactive nitrogen budget during the NASA SONEX Mission, *Geophys. Res. Lett.*, 26, 3057-3060, <https://doi.org/10.1029/1999GL900589>, 1999.
- 775 Thomas, K., Berg, M., Boulanger, D., Houben, N., Gressent, A., Nédélec, P., Pätz, H.-W., Thouret, V., and Volz-Thomas, A.: Climatology of NO_y in the troposphere and UT/LS from measurements made in MOZAIC, *Tellus B*, 67, 28793, 10.3402/tellusb.v67.28793, 2015.
- 780 Thompson, C. R., Wofsy, S. C., Prather, M. J., Newman, P. A., Hanisco, T. F., Ryerson, T. B., Fahey, D. W., Apel, E. C., Brock, C. A., Brune, W. H., Froyd, K., Katich, J. M., Nicely, J. M., Peischl, J., Ray, E., Veres, P. R., Wang, S., Allen, H. M., Asher, E., Bian, H., Blake, D., Bourgeois, I., Budney, J., Bui, T. P., Butler, A., Campuzano-Jost, P., Chang, C., Chin, M., Commane, R., Correa, G., Crounse, J. D., Daube, B., Dibb, J. E., Digangi, J. P., Diskin, G. S., Dollner, M., Elkins, J. W., Fiore, A. M., Flynn, C. M., Guo, H., Hall, S. R., Hannun, R. A., Hills, A., Hints, E. J., Hodzic, A., Hornbrook, R. S., Huey, L. G., Jimenez, J. L., Keeling, R. F., Kim, M. J., Kupe, A., Lacey, F., Lait, L. R., Lamarque, J.-F., Liu, J., Mckain, K., Meinardi, S., Miller, D. O., Montzka, S. A., Moore, F. L., Morgan, E. J., Murphy, D. M., Murray, L. T., Nault, B. A., Neuman, J. A., 785 Nguyen, L., Gonzalez, Y., Rollins, A., Rosenlof, K., Sargent, M., Schill, G., Schwarz, J. P., St. Clair, J. M., Steenrod, S. D., Stephens, B. B., Strahan, S. E., Strode, S. A., Sweeney, C., Thames, A. B., Ullmann, K., Wagner, N., Weber, R., Weinzierl, B., Wennberg, P. O., Williamson, C. J., Wolfe, G. M., and Zeng, L.: The NASA Atmospheric Tomography (ATom) Mission: Imaging the chemistry of the global atmosphere, *B. Am. Meteorol. Soc.*, 1-53, 10.1175/bams-d-20-0315.1, 2021.
- 790 Toon, O. B., Maring, H., Dibb, J., Ferrare, R., Jacob, D. J., Jensen, E. J., Luo, Z. J., Mace, G. G., Pan, L. L., Pfister, L., Rosenlof, K. H., Redemann, J., Reid, J. S., Singh, H. B., Thompson, A. M., Yokelson, R., Minnis, P., Chen, G., Jucks, K. W., and Pszenny, A.: Planning, implementation, and scientific goals of the Studies of Emissions and Atmospheric Composition, Clouds and Climate Coupling by Regional Surveys (SEAC⁴RS) field mission, *J. Geophys. Res.- Atmos.*, 121, 4967-5009, 10.1002/2015jd024297, 2016.
- 795 Travis, K. R., Nault, B. A., Crawford, J. H., Bates, K. H., Blake, D. R., Cohen, R. C., Fried, A., Hall, S. R., Huey, L. G., Lee, Y. R., Meinardi, S., Min, K. E., Simpson, I. J., and Ullman, K.: Impact of improved representation of VOC emissions and production of NO_x reservoirs on modeled urban ozone production, *Atmos. Chem. Phys.*, 2024, 1-27, 10.5194/egusphere-2024-951, 2024.
- 800 Travis, K. R., Jacob, D. J., Fisher, J. A., Kim, P. S., Marais, E. A., Zhu, L., Yu, K., Miller, C. C., Yantosca, R. M., Sulprizio, M. P., Thompson, A. M., Wennberg, P. O., Crounse, J. D., St. Clair, J. M., Cohen, R. C., Laughner, J. L., Dibb, J. E., Hall, S. R., Ullmann, K., Wolfe, G. M., Pollack, I. B., Peischl, J., Neuman, J. A., and Zhou, X.: Why do models overestimate surface ozone in the Southeast United States?, *Atmos. Chem. Phys.*, 16, 13561-13577, 10.5194/acp-16-13561-2016, 2016.
- 805 Travis, K. R., Heald, C. L., Allen, H. M., Apel, E. C., Arnold, S. R., Blake, D. R., Brune, W. H., Chen, X., Commane, R., Crounse, J. D., Daube, B. C., Diskin, G. S., Elkins, J. W., Evans, M. J., Hall, S. R., Hints, E. J., Hornbrook, R. S., Kasibhatla, P. S., Kim, M. J., Luo, G., McKain, K., Millet, D. B., Moore, F. L., Peischl, J., Ryerson, T. B., Sherwen, T., Thames, A. B., Ullmann, K., Wang, X., Wennberg, P. O., Wolfe, G. M., and Yu, F.: Constraining remote oxidation capacity with ATom observations, *Atmos. Chem. Phys.*, 20, 7753-7781, 10.5194/acp-20-7753-2020, 2020.
- 810 Volz-Thomas, A., Berg, M., Heil, T., Houben, N., Lerner, A., Petrick, W., Raak, D., and Pätz, H. W.: Measurements of total odd nitrogen (NO_y) aboard MOZAIC in-service aircraft: instrument design, operation and performance, *Atmos. Chem. Phys.*, 5, 583-595, 10.5194/acp-5-583-2005, 2005.
- 815 Weinheimer, A. J.: Chemical Methods: Chemiluminescence, Chemical Amplification, Electrochemistry, and Derivation, in: *Analytical Techniques for Atmospheric Measurement*, 311-360, <https://doi.org/10.1002/9780470988510.ch7>, 2006.



Weinheimer, A. J., Walega, J. G., Ridley, B. A., Gary, B. L., Blake, D. R., Blake, N. J., Rowland, F. S., Sachse, G. W., Anderson, B. E., and Collins, J. E.: Meridional distributions of NO_x , NO_y , and other species in the lower stratosphere and upper troposphere during AASE II, *Geophys. Res. Lett.*, 21, 2583-2586, <https://doi.org/10.1029/94GL01897>, 1994.

- 820 Worden, H. M., Bowman, K. W., Kulawik, S. S., and Aghedo, A. M.: Sensitivity of outgoing longwave radiative flux to the global vertical distribution of ozone characterized by instantaneous radiative kernels from Aura-TES, *J. Geophys. Res.*, 116, 10.1029/2010jd015101, 2011.
- Zahn, A., Brenninkmeijer, C. A. M., Asman, W. A. H., Crutzen, P. J., Heinrich, G., Fischer, H., Cuijpers, J. W. M., and van Velthoven, P. F. J.: Budgets of O_3 and CO in the upper troposphere: CARIBIC passenger aircraft results 1997–2001, *J. Geophys. Res.-Atmos.*, 107, ACH 6-1-ACH 6-20, <https://doi.org/10.1029/2001JD001529>, 2002.
- 825